Technical Report Documentation Page

1. Report No.	2. Government Accession No.	3. Recipient's Catalog No.
SWUTC/14/600451-00076-1		

4. Title and Subtitle	5. Report Date
FATIGUE AND FRACTURE PROPERTIES OF AGED BINDERS IN THE CONTEXT OF RECLAIMED ASPHALT MIXES	August 2014
	6. Performing Organization Code

7. Author(s)	8. Performing Organization Report No.
Arash Motamed, Solomon Nyanhongo, Pravat Karki, and Amit Bhasin	

9. Performing Organization Name and Address	10. Work Unit No. (TRAIS)
Center for Transportation Research University of Texas at Austin 1616 Guadalupe Street, Suite 4.200 Austin, Texas 78701	11. Contract or Grant No. DTRT12-G-UTC06

12. Sponsoring Agency Name and Address	13. Type of Report and Period Covered
Southwest Region University Transportation Center Texas A&M Transportation Institute Texas A&M University System College Station, Texas 77843-3135	Final Report
	14. Sponsoring Agency Code

15. Supplementary Notes

Project supported by a grant from the U.S. Department of Transportation, University of Transportation Centers Program, and general revenues from the State of Texas.

Project title: Micro Crack Growth in Recycled Asphalt Mixtures

16. Abstract

Evidence in the literature indicates that the stiffness of the asphalt binder increases and ductility of the binder decreases with oxidative aging. Typically for unmodified asphalt binders, increase in stiffness or decrease in ductility is regarded as detrimental to the fatigue cracking or fracture resistance of the asphalt binder. However, fundamentally the stiffness of the binder and its strength are two different attributes that may not necessarily be related to each other. There is very little information in the literature that relates the fatigue cracking resistance or strength of the asphalt binder to the extent of oxidative aging. This information is not only important to assess the durability and cracking life of asphalt pavements but is also very important in the context of reclaimed asphalt pavements (RAP). The use of RAP not only reduces the waste produced from milling and removing the asphalt pavement layers at the end of their service life, but also reduces the amount of asphalt required for the construction of new roadways. In an effort to improve sustainable practices associated with pavement constructions, state DOTs have been gradually increasing the allowable percentage of RAP in new asphalt mixtures over the last two decades. However, the asphalt binder in RAP is highly oxidized and is deemed to be susceptible to load related fatigue cracking. The focus of this study was to investigate the effect of asphalt binder oxidation on its fracture properties and fatigue cracking performance. To this end, fatigue cracking resistance of an asphalt binder was measured at different levels of aging using a standardized glass bead composite. The glass bead composite simulates the stress state that asphalt binders experience in the field, while it excludes aggregate-asphalt binder interactions. Furthermore, this research also investigated the effect of aging on fracture properties of an asphalt binder by conducting monotonic fracture tests using a poker chip test geometry. The findings from this study provide a better understanding of the effect of aging on the fracture and fatigue properties of asphaltic materials.

17. Key Words	18. Distribution Statement
Reclaimed Asphalt Pavements, RAP, Oxidation, Oxidative Aging	No restrictions. This document is available to the public through NTIS: National Technical Information Service 5285 Port Royal Road Springfield, Virginia 22161

19. Security Classif.(of this report)	20. Security Classif.(of this page)	21. No. of Pages	22. Price
Unclassified	Unclassified	55	

FATIGUE AND FRACTURE PROPERTIES OF AGED BINDERS IN THE CONTEXT OF RECLAIMED ASPHALT MIXES

by

Arash Motamed, Ph.D.
Post-doctoral Research Assistant

Solomon Nyanhongo
Undergraduate Research Assistant

Pravat Karki
Graduate Research Assistant

and

Amit Bhasin, Ph.D.
Associate Professor

Southwest Region University Transportation Center
Center for Transportation Research
Department of Civil, Architectural, and Environmental Engineering
The University of Texas at Austin
Austin, Texas 78712

SWUTC/14/600451-00076-1

Micro Crack Growth in Recycled Asphalt Mixtures

August 2014

DISCLAIMER

The contents of this report reflect the views of the authors, who are responsible for the facts and the accuracy of the information presented herein. This document is disseminated under the sponsorship of the Department of Transportation, University Transportation Centers Program, in the interest of information exchange. Mention of trade names or commercial products does not constitute endorsement or recommendations for use.

ACKNOWLEDGMENTS

The authors recognize that support was provided by a grant from the U.S. Department of Transportation, University Transportation Centers Program to the Southwest Region University Transportation Center which is funded, in part, with general revenue funds from the State of Texas. The authors would like to acknowledge Dr. Yong-Rak Kim from University of Nebraska-Lincoln, for serving as a Project Monitor for this study.

ABSTRACT

Evidence in the literature indicates that the stiffness of the asphalt binder increases and ductility of the binder decreases with oxidative aging. Typically for unmodified asphalt binders, increase in stiffness or decrease in ductility is regarded as detrimental to the fatigue cracking or fracture resistance of the asphalt binder. However, fundamentally the stiffness of the binder and its strength are two different attributes that may not necessarily be related to each other. There is very little information in the literature that relates the fatigue cracking resistance or strength of the asphalt binder to the extent of oxidative aging. This information is not only important to assess the durability and cracking life of asphalt pavements but is also very important in the context of reclaimed asphalt pavements (RAP). The use of RAP not only reduces the waste produced from milling and removing the asphalt pavement layers at the end of their service life, but also reduces the amount of asphalt required for the construction of new roadways. In an effort to improve sustainable practices associated with pavement constructions, state DOTs have been gradually increasing the allowable percentage of RAP in new asphalt mixtures over the last two decades. However, the asphalt binder in RAP is highly oxidized and is deemed to be susceptible to load related fatigue cracking. The focus of this study was to investigate the effect of asphalt binder oxidation on its fracture properties and fatigue cracking performance. To this end, fatigue cracking resistance of an asphalt binder was measured at different levels of aging using an standardized glass bead composite. The glass bead composite simulates the stress state that asphalt binders experience in the field, while it excludes aggregate-asphalt binder interactions. Furthermore, this research also investigated the effect of aging on fracture properties of an asphalt binder by conducting monotonic fracture tests using a poker chip test geometry. The findings from this study provide a better understanding of the effect of aging on the fracture and fatigue properties of asphaltic materials.

EXECUTIVE SUMMARY

Over the last two decades, the use of reclaimed asphalt pavements (RAP) as a construction material has significantly increased. This increase in the use of RAP materials is aligned with the concept of sustainable transportation infrastructure and is also motivated by the cost savings that are realized by incorporating RAP in new asphalt mixtures. Despite all the benefits associated with the use of RAP, the inclusion of higher percentages of RAP in a fresh asphalt mixture results in increased mixture stiffness. This increased stiffness is considered to result in an increased susceptibility to fatigue and low-temperature cracking. The objective of this study was to investigate the former, i.e. whether or not aged asphalt binders have poor fracture or fatigue cracking resistance when subjected to similar external loading conditions at intermediate temperatures.

In order to achieve the overall goal of this study, fatigue cracking and fracture resistance of a selected asphalt binder were measured at different levels of aging. To age asphalt binders in the laboratory at different levels, two different aging devices were used: the rolling thin film oven (RTFO), and pressure aging vessel (PAV). The RTFO simulates the short-term aging due to construction (production and placement), and the PAV simulates the long-term aging due to construction and service. Furthermore, to simulate the extended aging, the PAV-aged asphalt binder was further aged using the PAV for a second and third time. Finally to simulate the binder in a HMA containing RAP, the RTFO-aged binder was mixed with the double PAV-aged binder in two different proportions that represent the typical percentage of RAP use. Fatigue cracking resistance was measured using a standardized glass bead composite. The glass bead composite simulates the stress state that asphalt binders experience in the field, while it excludes aggregate-asphalt binder interactions. After aging the binder and fabricating the standardized glass bead composites, the mechanical (undamaged and fatigue) properties of the asphalt binder were measured. These measurements included the mechanical properties of asphalt binder at different levels of aging and also glass-bead mixtures with different percentage of RAP. Continuum damage mechanics was used to analyze the results from the fatigue tests. Fracture properties of the asphalt binder at different levels of aging or RAP content were measured using a poker chip geometry.

The results from this study show that aging causes the asphalt binder and concomitant composite to become more stiff and relatively less time dependent. This finding was expected based on the current understanding of the binder behavior after aging. However, it was also observed that the viscous component of the complex shear modulus of the binder

(in the standardized composite), reflected by the parameter $G^{*}Sin\delta$, did not change significantly with aging. The results from fatigue test using the standardized glass bead composite subjected to stress controlled cyclic load, clearly demonstrated that the fatigue cracking resistance of asphalt binder increased with aging. The results from thin film fracture test illustrate that both maximum tensile stress and fracture energy increase until some level of aging. The results also demonstrate that the mechanical properties and performance of the mix containing RAP reflect a composite effect of its components. In summary, the findings from this work suggest that although aged binder and concomitant RAP mixes may have higher stiffness due to aging, these materials also tend to show an increased fracture and fatigue cracking resistance. Consequently, both of these factors must be considered in order to fully optimize mix designs containing RAP and maximize the use of these materials.

TABLE OF CONTENTS

List of Figures **xi**

Chapter 1. Introduction **1**

1.1 Project Background 1

1.2 Objectives 2

1.3 Report Structure 3

Chapter 2. Background and Research Approach **5**

2.1 Use of reclaimed asphalt in new pavement construction 5

2.2 Overview of Fatigue and Fracture of Asphalt Binders 7

2.3 Recently Developed Methods 9

2.3.1 Linear amplitude sweep test 9

2.3.2 Thin film fracture test 9

2.3.3 Binder-glass bead mortar test 9

2.3.4 Fine aggregate mortar test 10

2.4 Theoretical Background of Analysis Method 10

2.4.1 Linear viscoelastic constitutive model 11

2.4.2 Schapery's Extended Correspondence Principles 11

2.4.3 Thermodynamic-based Work Potential Theory 14

2.4.4 Rate-type Damage Evolution Law 15

2.5 Research Approach 16

Chapter 3. Materials **19**

3.1 Material selection and preparation 19

3.2 Specimen fabrication for standardized composite test 19

3.3 Specimen fabrication for thin film fracture test 24

Chapter 4. Test Methods, Analysis and Results **27**

4.1 Standardized composite test 27

4.1.1 Linear viscoelastic properties 27

4.1.2 Fatigue behavior 32

4.2 Thin Film Fracture Test 34

Chapter 5. Summary of Findings **39**

References **41**

LIST OF FIGURES

Figure 2.1. Schematic of stress - strain relationship in viscoelastic and pseudo-elastic domains . . . 13
Figure 3.1. Aging procedure and stages used in this study. . . . 20
Figure 3.2. Gradation of glass beads used to produce specimens for standardized composite test . . . 21
Figure 3.3. Manually mixing glass beads with the asphalt binder to prepare a homogenous mixture . . . 22
Figure 3.4. Manufactured mold assembly for compaction . . . 22
Figure 3.5. Glass bead mixture being poured into the mold and compacted using the rod and drop weight . . . 23
Figure 3.6. A test specimen and the test setup in Dynamic Shear Rheometer . 24
Figure 3.7. Thin film fracture test set-up . . . 25
Figure 4.1. Creep and recovery test results for PAV3 aged binder under 5 and 10 kPa stress levels . . . 28
Figure 4.2. Measured creep compliance for PAV-3 aged binder under different stress levels at 20°C . . . 28
Figure 4.3. Power law estimation of the creep response for PAV3 aged binder under a constant load of 5 kPa at 20°C . . . 29
Figure 4.4. Coefficient of the time-dependent term in the power law equation or J_1 for different levels of aging at 20°C . . . 30
Figure 4.5. The exponent in the power law equation or m-value for different levels of aging at 20°C . . . 31
Figure 4.6. Linear viscoelastic dynamic shear modulus for different levels of aging at 10Hz and 20°C . . . 31
Figure 4.7. Linear viscoelastic phase angle for different levels of aging at 10Hz and 20°C . . . 32
Figure 4.8. Fatigue parameter ($G^{*}Sin\delta$) for different levels of aging at 20°C . 32
Figure 4.9. Fatigue test results for PAV3 aged binder at 330 kPa, 20°C, and 10 Hz . . . 33
Figure 4.10. Typical damage evolution curve (C vs S) obtained for PAV3 aged binder . . . 34

Figure 4.11. Fatigue life (cycles required for reaching to 50% of initial modulus) for different levels of aging 34
Figure 4.12. Monotonic fracture test results for PAV aged binder at the rate of 1micrometer/second 35
Figure 4.13. Comparison of the fracture behavior of the tested asphalt binder at different levels of aging 36
Figure 4.14. Comparison of the maximum tensile stress for different levels of binder aging 36
Figure 4.15. Comparison of the fracture energy for different levels of binder aging 37

CHAPTER 1. INTRODUCTION

1.1 PROJECT BACKGROUND

Aging of asphalt binders is known to influence the properties of the asphalt mixtures during the construction and subsequent service life of the pavement. Changes in material properties due to aging are also regarded as one of the main causes of pavement deterioration. There is significant evidence in the literature that indicates that oxidative aging increases the stiffness of the asphalt binder and decreases the ductility of the binder. Typically for unmodified asphalt binders an increase in stiffness or decrease in ductility is regarded as detrimental to the fatigue cracking or fracture resistance of the asphalt binder. However, fundamentally the stiffness of the binder and its strength are two different attributes that may not necessarily be related to each other. There is very little information in the literature that relates the fatigue cracking resistance or strength of the asphalt binder to the extent of oxidative aging. This information is not only important to assess the durability and cracking life of asphalt pavements but is also very important in the context of reclaimed asphalt pavements (RAP).

Over the last two decades, the use of reclaimed asphalt pavements (RAP) as a construction material has significantly increased. This increase in the use of RAP materials is aligned with the concept of sustainable transportation infrastructure and is also motivated by the cost savings that are realized by incorporating RAP in new asphalt mixtures. The use of RAP not only reduces the waste produced from milling and removing asphalt pavement layers at the end of their service life, but also reduces the amount of asphalt required during the construction of new roadways. Therefore, RAP technology is an important element in building and maintaining environment friendly roadways. In an effort to reduce costs and improve sustainable practices associated with pavement construction, state DOTs have been gradually increasing the allowable percentage of RAP in new asphalt mixtures. Despite all the benefits associated with the use of RAP, there are some questions related to the long-term durability of asphalt mixtures containing large percentages of RAP. Asphalt mixtures and pavements rely on the inherent ability of the asphalt binder to relax internal stresses that build up at low temperatures, thus preventing formation of transverse cracks. The ductile behavior of asphalt binder is also important to prevent nucleation and rapid propagation of fatigue cracks when subjected to cyclic loading due to traffic. The asphalt binder in RAP is highly oxidized and has a reduced ability to relax compared to fresh asphalt binder. While the reduced ability of the binder to relax translates into higher stress accumulation (particularly as the pavement temperature drops) it does not necessarily translate into increased susceptibility of the binder to crack or fail. In particular, cracking in the binder is governed by not just the stresses experienced by the material but also by the tensile strength of the material to resist such stresses. Traditionally, a lot of attention has been paid in the binder industry to evaluate the stiffness and stresses that are developed in aged and unaged binder but such information is only of value when juxtaposed against the changes in the strength of the material.

1.2 OBJECTIVES

The main objective of this study is to evaluate the effect of aging on the fatigue cracking resistance of asphalt binders at an intermediate temperature. In this study, we will use a standardized glass bead composite to measure the fatigue properties of an asphalt binder at different levels of aging. The glass bead composite simulates the stress state that asphalt binders experience within HMA, while it excludes aggregate-asphalt binder interactions. Note that the aggregate-asphalt interactions are excluded by design not because such interactions are not important in the real world but rather to facilitate a systematic study of the asphalt binder in isolation. To age asphalt binders in the laboratory at different levels, two different aging devices were used: the rolling thin film oven (RTFO), and pressure aging vessel (PAV). The RTFO simulates the short-term aging due to construction (production and placement), and the PAV simulates the long-term aging due to construction and service. Furthermore, to simulate the extended aging, the PAV-aged asphalt binder was further aged using the PAV for a second and third time. Finally to simulate the binder in a HMA containing RAP, the RTFO-aged binder was mixed with the double PAV-aged binder in two different proportions that represent the typical percentage of RAP use. After aging the binder and fabricating the standardized glass bead composites, the mechanical (undamaged and fatigue) properties of the asphalt binder were measured. These measurements included the mechanical properties of asphalt binder at different levels of aging and also glass-bead mixtures with different percentage of RAP. Continuum damage mechanics was used to analyze the results from the fatigue tests. The second objective of this study was to measure the fracture properties of the asphalt binder at different levels of aging or RAP content. The poker chip geometry was used to measure the fracture properties of the aged asphalt binder at an intermediate temperature. The findings from this study provide a better understanding of the long term performance of aged binders as in the case of RAP.

1.3 REPORT STRUCTURE

Chapter 2 of this report presents a background on the need for improving our understanding of aging and its effect on the fatigue properties of asphaltic materials. This chapter also reviews the test methods that are available to characterize the fatigue and fracture properties of asphalt binders with an emphasis on viscoelastic continuum damage. Chapter 3 presents a description of the materials that were selected and used in this study along with a detailed description of the procedures that were used to fabricate the test specimens. This is followed by a description of the various test methods that were used in this study and a detailed analysis of the test results in Chapter 4. Finally, Chapter 5 presents concluding remarks based on the findings from this study.

CHAPTER 2. BACKGROUND AND RESEARCH APPROACH

Oxidative aging can significantly change the behavior of asphalt binders and composites over time. It is well established in the literature that aging influences the properties of an asphalt binder and consequently that of the asphalt mixture during construction and over the service life of the pavement. For example, several research studies have demonstrated that the stiffness of the asphalt binder increases and ductility of the binder decreases with oxidative aging. Typically for unmodified asphalt binders an increase in stiffness or decrease in ductility is regarded as detrimental to the fatigue cracking or fracture resistance of the asphalt binder. However, fundamentally the stiffness of the binder and its strength are two different attributes that may not necessarily be related to each other. As mentioned earlier, there is very little information in the literature that relates the fatigue cracking resistance or strength of the asphalt binder to the extent of oxidative aging. This information is not only important to assess the durability and cracking life of asphalt pavements but is also very important in the context of recycled asphalt pavements (RAP). This chapter briefly reviews the importance knowing the effect of aging or use aged materials in the performance of asphaltic materials. Furthermore, the approaches to measure the fatigue and fracture of asphaltic materials will be reviewed with the intention of selecting the most promising approaches.

2.1 USE OF RECLAIMED ASPHALT IN NEW PAVEMENT CONSTRUCTION

Reclaimed asphalt pavement (RAP) refers to asphalt material that is typically recovered from milled asphalt pavements at the end of their service life. In general, the techniques for recycling asphalt pavement can be categorized in five groups (Decker, 1997): cold planning, hot recycling, hot in-place recycling, cold in-place recycling, and full depth reclamation. The focus of this study is hot recycling, since it is more commonly used in the United States. Hot recycling mixes RAP with virgin asphalt binder and aggregate to produce a new hot mix asphalt (HMA). In practice, either a drum or batch type hot mix plant can be used to produce a HMA with RAP, although the former is more common. A HMA incorporating RAP is placed and compacted in a manner that is similar to virgin HMA. The use of RAP in fresh HMA:

- reduces the waste produced from milling and removing asphalt pavement layers at the end of their service life,

- reduces the amount of asphalt binder required during construction, and
- reduces the construction costs related to the asphalt binder and aggregate.

Due to the above economic and environmental advantages, the use of RAP in HMA has been growing steadily over the last several years. During the last two decades, several research studies have been conducted to better understand the effect of aging or the effect of RAP on the mechanical properties of the HMA. These research studies demonstrate that the asphalt binder associated with the RAP material is heavily aged and hardened mainly due to six major mechanisms (Roberts et al., 1996; Tyrion, 2000; Karlsson and Isacsson, 2006):

- oxidation,
- volatilization,
- polymerization,
- thixotropy,
- syneresis, and
- separation.

Therefore, producing mixtures using RAP will result in stiffer and less viscous pavements, compared to the pavements made using virgin HMA. Although the change in HMA properties due to aging improves the early-age performance of HMA such as rutting resistance, but it is also widely believed that this might make pavements more prone to the fatigue cracking. Thus, despite all the benefits associated with the use of RAP, there are some questions related to the long-term durability of asphalt mixtures containing higher percentages of RAP. In general, the ductile behavior of asphalt binder is important to prevent nucleation and rapid propagation of fatigue cracks when subjected to cyclic loading due to traffic. Since the asphalt binder in RAP is highly oxidized and does not have the ability to relax, the fatigue cracking and low temperature cracking resistance of asphalt mixtures containing a high percentage of RAP are a concern. Strategies such as high temperatures to better homogenize the old and recycled binder and the use of rejuvenators are often employed to improve the performance of the asphalt mixture with RAP. However, the efficacy of such strategies is dependent on the specific combination of materials used. Therefore, there is a need to clearly quantify the effect of oxidation and the use of RAP on crack nucleation and crack growth in asphalt composites.

2.2 OVERVIEW OF FATIGUE AND FRACTURE OF ASPHALT BINDERS

It is well established that oxidative aging results in stiffer binder. However, in addition to measuring stiffness and the ability to relax, the main goal of this study was to characterize the fatigue and fracture resistance properties of the asphalt binder as a function of aging. To this end, this section reviews some of the methods and metrics that are currently in use or have been recently developed to characterize the fatigue and fracture resistance of an asphalt binder.

According to the current PG specification (AASHTO M-320), a binder is deemed as resistant to fatigue cracking at intermediate temperatures if the parameter $G^{*}Sin\delta$ of the PAV aged binder is less than 5000 kPa (G^{*} is the complex modulus and δ is the phase angle). In this case, intermediate temperature is defined as 4Â°C above the average of the high and low temperatures. This parameter is measured using a DSR and by applying a sinusoidal loading at the frequency of 10 radians/second. Just as in the case of high temperature grade, this specification is based on neat asphalt binders. This specification is based on the premise that a stiffer asphalt binder is more susceptible to fatigue and low temperature cracking. This premise implicitly assumes that all asphalt binders have similar tensile strength. In other words, a major drawback of this specification is that it is based on the stiffness of the binder and not the strength of the binder. Fatigue cracking is the incremental nucleation and growth of microcracks. It is important to accurately estimate the strength of the asphalt binder in order to characterize its ability to resist fatigue cracking.

As a simplified analogy, consider two different binders with similar tensile strength. In this case, when both binders are subjected to the similar tensile strains, the material with higher stiffness would result in a higher stress to strength ratio. Consequently, the material with the higher stiffness would be more prone to fatigue cracking. The rationale for using the current specification criterion for asphalt binders is somewhat similar to this analogy. However, the SHRP research was conducted on mostly unmodified asphalt binders. Over the last two decades, asphalt binder producers have started producing asphalt binders using chemical and physical modifiers (e.g., poly phosphoric acid and polymers). In addition, users of the asphalt binders have increased the use of other modifiers such as liquid anti strip agent for moisture resistance and waxes and surfactants to produce warm asphalt mixtures. Several of these modifications are likely to change the strength properties of the asphalt binder as well. Consequently, the linear elastic or viscoelastic properties of the binder are unlikely to be an accurate reflection of the strength of the material.

Bahia et al. (2010) reported a poor correlation between $G^{*}Sin\delta$ and fatigue cracking of HMA pavements. Similar findings were reported by other researchers along with suggested alternatives to replace the $G^{*}Sin\delta$ as a specification for resistance to fatigue crack growth (Olard and Di Benedetto, 2004; Andriescu and Hesp, 2009). In a recent study, Arega et al. (2011) measured $G^{*}Sin\delta$ for several different modified and unmodified binders including binders that were modified using WMA additives. They compared $G^{*}Sin\delta$ to the tensile strength of the asphalt binders and reported that there was very little correlation between stiffness and tensile strength of the asphalt binders. Note that the tensile strength governs the fatigue crack growth process although the relationship between the tensile strength and fatigue crack growth may be influenced by modification process. In fact, in many cases, tensile strength of the binder increased with an increase in stiffness suggesting an improvement in the fatigue cracking resistance when subjected to similar stress conditions. However, it is clear from the results that certain binders that had a low $G^{*}Sin\delta$ and easily met the specification limit for $G^{*}Sin\delta < 5000$ kPa also had a low tensile strength as well and vice-versa.

Ongoing studies attempt to rectify the shortcomings of the $G^{*}Sin\delta$ by using other approaches to test the asphalt binder with a dynamic shear rheometer (DSR). Two approaches in particular are the time sweep test and the amplitude sweep test. Anderson et al. (2001) reported that the use of a DSR for a time sweep test on asphalt binder specimens with a parallel plate geometry may result in artifacts that may resemble fatigue failure. Subsequently, Planche et al. (2004) reported that several artifacts that look like fatigue damage in the mechanical response can be corrected to obtain the true fatigue behavior of the asphalt binder. Bahia and co-workers have proposed the linear amplitude sweep test (LAS) to measure the fatigue cracking resistance of asphalt binders. This test requires that a sample of the binder be subjected to sinusoidal loading in a DSR (similar to the current method). After a specific number of cycles the applied stress amplitude is increased and the process is repeated until the stress amplitude is high enough to cause damage in the specimen. Johnson (2010) conducted the LAS test on materials from several LTPP test sections and compared the results to the amount of cracking observed in the pavement. The results were promising despite the fact that differences in strain levels due to differences in pavement structures would also play a role in the overall cracking observed in the pavement sections. The subsequent sections present an overview of the recent methods that have been developed to characterize the fatigue and fracture properties of asphalt binders.

2.3 RECENTLY DEVELOPED METHODS

2.3.1 Linear amplitude sweep test

This test is typically conducted by applying a strain controlled cyclic load to a 1 mm thick binder specimen, between parallel plates, using a DSR (Bahia et al., 2010). The applied strain amplitude is linearly increased after every 100 cycles. The resulting shear stress is recorded and analyzed to quantify the fatigue cracking potential. A creep-recovery test or a frequency sweep test at low stress or strain amplitudes is also typically conducted prior to the LAS in order to obtain the linear viscoelastic properties of the binder. The linear viscoelastic properties are then used along with the data obtained from the LAS to compute the damage parameters.

2.3.2 Thin film fracture test

Both the linear amplitude sweep test and the monotonic fracture test are typically conducted on bulk specimens of asphalt binders in shear. However, asphalt binders within asphalt mixtures are confined between relatively rigid aggregate particles. This confinement results in very high hydrostatic stresses and significantly improved tensile strength, similar to thin films of adhesives between rigid substrates. As a result, it is important to consider the stress state of the asphalt binder when investigating fatigue or fracture properties. The thin film fracture test is a direct tension test that is conducted on a thin film of asphalt binder. In this test, a constant rate (monotonic) displacement is applied in direct tension on a thin film of asphalt binder between two metal substrates until failure. The test can be conducted at different rates of loading and the load versus deformation curve can be used to characterize the inherent fracture resistance of the asphalt binder. This test can also be conducted using cyclic loading to simulate fatigue cracking in the asphalt binder specimen.

2.3.3 Binder-glass bead mortar test

The stress state that a binder experiences in a mixture can be simulated in a mortar specimen, i.e., binder mixed with sand sized and finer aggregates. However, it is also important to avoid the influence of aggregates in evaluating the inherent fracture resistance of asphalt binders. This is especially true if a test is to serve the purpose of a binder purchase specification in future. Therefore, this test utilizes a standard material such as glass beads to fabricate the mortar specimen. In a typical test, a mortar specimen is fabricated using a mixture of asphalt binder and glass beads of various sizes. The specimen uses glass beads of sizes 1mm, 0.5mm, and 0.1mm following close to dense graded line. The test can be conducted by applying either a monotonically increasing shear stress or cyclic loading with a constant shear stress or strain amplitude. Since the fatigue damage that occurs in a composite can be treated to be distributed over space, the viscoelastic continuum damage (VECD) principles can be used to extract the true fatigue characteristics of the specimen irrespective of the rate and mode of loading (continuous or cyclic). This theory has been successfully used in another study in which the test specimen was subject to cyclic torsion at different stress or strain amplitudes (Motamed et al., 2013).

2.3.4 Fine aggregate mortar test

This test is the same as the binder-glass bead mortar test, except that the glass beads are replaced with the mineral aggregates corresponding to a specific asphalt mixture (Kim et al., 2003, 2006; Palvadi et al., 2012; Karki et al., 2014a).

2.4 THEORETICAL BACKGROUND OF ANALYSIS METHOD

One of the challenges with conducting fatigue tests using binder samples with different levels of aging is that the stiffness of these binders varies significantly with aging. As a result, it is sometimes impractical to use the same level of loading conditions to conduct tests on a suite of materials with very different stiffness. For example, a high stress amplitude in a cyclic fatigue test would result in an extremely short fatigue life for the soft unaged or only short-term aged binder. On the other hand a low stress amplitude in a cyclic fatigue test would result in extremely high fatigue life for the stiff long-term aged binder (and an unrealistically long test duration). Conducting tests at different stress amplitudes would not allow for a direct comparison between the different materials. Similarly, tests conducted using a constant strain amplitude as an input would yield fatigue lives that are not an accurate representation of the material response under traffic loading. For example, under a given traffic load the stiffer binder would experience smaller strains compared to the softer binder. Therefore, for this study it was important to adopt a method of analysis to compare the damage resistance of different asphalt binders that is independent of the mode and amplitude of loading. Based on a review of the literature the viscoelastic continuum damage method was considered to be an appropriate analytical tool to evaluate the test data.

2.4.1 Linear viscoelastic constitutive model

The response of asphalt materials (asphalt cements and composites) differs with applied stress and strain rates, magnitudes and temperatures. Viscoelastic continuum damage (VECD) mechanics is extensively used to model the damage response of asphalt materials in a form that extracts the damage resistance of the material that is independent of the mode and amplitude of loading. This section presents the necessary background required to understand linear viscoelastic responses, the use of correspondence principles and work potential theory as required for VECD damage and healing models.

The linear viscoelastic property of an asphalt material represents its time- or rate-dependent mechanical response at low stresses or strains that does not induce damage to the material. In torsional shear mode of loading, the physical stress (τ) and the physical strain (γ) at time t are expressed in terms of convolution integrals, wherein $G(t)$ and $J(t)$ represent relaxation modulus and creep compliance in shear, and ξ represent the time variable.

$$\tau(t) = \int_0^t G(t-\xi,t)\,\frac{\partial\gamma(\xi)}{\partial\xi}d\xi \tag{2.1}$$

$$\gamma(t) = \int_0^t J(t-\xi,t)\,\frac{\partial\tau(\xi)}{\partial\xi}d\xi \tag{2.2}$$

As can be seen in these relations (equations 2.2 and 2.1) , one needs to know the relaxation or creep compliance of the material to quantify its stress or strain response. Researchers use mechanical (e.g. Maxwell, Wiechert, Kelvin, etc.) or phenomenological models (e.g. power law) to describe the relaxation or creep compliance of the material. Models that describe linear viscoelastic response of asphalt materials typically follow the time-temperature superposition principles, thereby facilitating computation of combined responses due to different loading and temperature conditions. The specific models that adequately described the linear viscoelastic properties of fine aggregate matrices used in this study are provided in corresponding sections of this report.

2.4.2 Schapery's Extended Correspondence Principles

Typical boundary value problems with viscoelastic materials can be solved by using Laplace transform or simple correspondence principles with the solutions for similar problems for linear elastic solids. However, such transformations are not applicable to problems wherein the traction or displacement boundary conditions change with time (e.g. crack growth or crack closing). To address such situations, Graham and Sabin (1973) presented the elastic-viscoelastic correspondence principles that Schapery (1984b) extended to solve viscoelastic problems in which the traction and displacement boundaries remain intact (CP-I) or change (CP-II and CP-III) with time. In summary, these extended principles transform the time-dependent stresses and strains in viscoelastic media into the time-independent stresses and strains of an equivalent or reference elastic material, and solve the viscoelastic problems in a pseudo-elastic domain. Schapery categorically provided the generalized expressions for such transformations in an earlier study (Schapery, 1984a). Researchers have applied Schapery's extended correspondence principles to describe asphalt material traction boundary value problems such as crack growth (Park and Schapery, 1997), fatigue damage (Lee and Kim, 1998; Park et al., 1996; Kim et al., 2003, 2006) and healing (Karki et al., 2014b) among many others.

In torsional shear tests performed for this part of the study, the selected modified correspondence principle, CP-II (Schapery, 1984a, 1989) transforms the viscoelastic shear variables into the pseudo-elastic variables (denoted by superscript, R) as follows:

$$\tau^R \equiv \tau \tag{2.3}$$

$$\gamma^R \equiv \frac{1}{G^R}\int_0^t G(t-\xi,t)\,\frac{\partial \gamma(\xi)}{\partial \xi}d\xi \tag{2.4}$$

The quantity, G^R used in these transformation expressions represents an arbitrary modulus in the transformed space, and is taken as unity in this study. The following inverse relations can transform the pseudo shear strain and pseudo shear stress back into time-dependent shear stress and shear strain (Kim and Little, 1990):

$$\tau \equiv \tau^R \tag{2.5}$$

$$\gamma \equiv G^R \int_0^t J(t-\xi,t)\,\frac{\partial \gamma^R(\xi)}{\partial \xi}d\xi \tag{2.6}$$

Using the extended correspondence principles, CP-II (Schapery, 1984a), and the steady state stress condition (Ferry, 1980; Tschoegl, 1989) for a material subjected to sinusoidal load, the amplitudes of pseudo shear stress and pseudo shear strain at the k^{th} load cycle can be given by these simplified relations (Underwood et al., 2010):

$$\tau_{oc,k}^{R} \equiv \frac{\beta+1}{2}\tau_{pp,k} \tag{2.7}$$

$$\gamma_{oc,k}^{R} \equiv \frac{\beta+1}{2}\left(\frac{\gamma_{pp,k}G_{LVE}^{*}}{G^{R}}\right) \tag{2.8}$$

The subscript oc refers to the peak amplitude of pseudo shear stress or the peak amplitude of pseudo shear strain that are responsible for fatigue cracking in the k^{th} shear load cycle; the subscript pp refers to corresponding peak-to-peak magnitude of viscoelastic shear stress and shear strain as shown in Figure 2.1. The notation, G_L^*VE in the pseudo shear strain definition refers to the linear viscoelastic dynamic shear modulus of the given material that is measured by applying a small level of strain or stress within the linear viscoelastic range of the material. Similarly, the parameter β refers to a correction factor to account for the portion of the stress-strain history that is responsible for crack growth in a given cycle (Underwood et al., 2010). The concept of such correction was also used in some earlier studies related to uniaxial load in which the researchers used half (Daniel, 2001) or quarter (Daniel and Kim, 2002) of stress-strain history. In a torsional shear test, the full portion of each load cycle is responsible for shear damage in the material. Due to symmetry, $\beta = 0$ is used to calculate the pseudo shear strain that is responsible for damage accumulation in each semi-cycle.

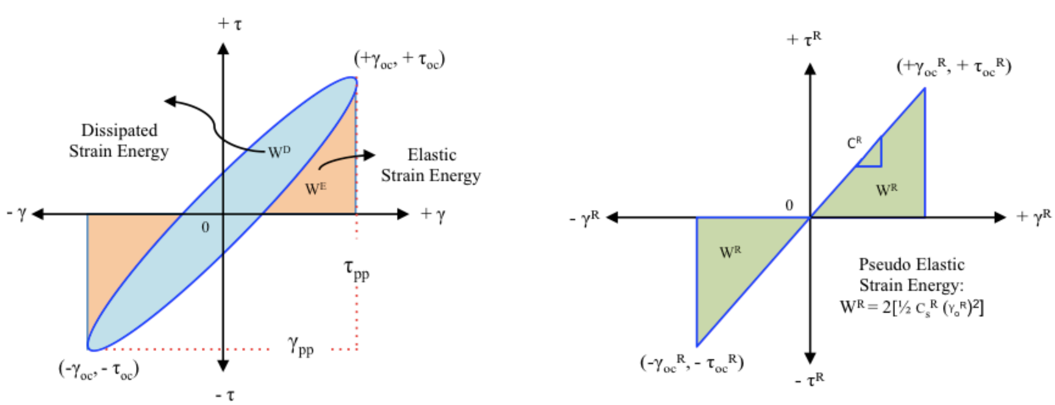

Figure 2.1. Schematic of stress - strain relationship in viscoelastic and pseudo-elastic domains

In a stress-controlled cyclic shear test, the shear stress amplitude divided by the shear strain amplitude at a given steady state load cycle yields the dynamic shear modulus of the material. In the pseudo-elastic realm, the secant slope of pseudo stress-strain curve is defined as the pseudo-stiffness of the material corresponding to that cycle:

$$C^R_{s,k}(S_s) \equiv \frac{\tau^R_{oc,k}}{\gamma^R_{oc,k}} \tag{2.9}$$

The value of pseudo-stiffness depends on the change in the internal state of the material (represented by S_s), and therefore is denoted as $C^R_{s,k}(S_s)$ wherein the subscript s refers to the shear mode of loading. A more robust method to compute pseudo-stiffness requires time-integration on the stress-strain history without assuming the steady state definition. Other researchers (Underwood et al., 2010) have also proposed a mixed use of time-integration to determine pseudo-stiffness based on transient effects. They have attributed this need to the transient effects due to the sudden application of damage-inducing load from zero. However, the sinusoidal shear tests conduced for this work resulted in very similar stress and strain amplitudes above and below a zero-mean axis in a given cycle, following a steady state response. Therefore, for the purpose of this study, the simplified definition of pseudo-stiffness as defined earlier was used, wherein a correction factor (I) accounts for sample-to-sample variability.

$$C^R_{s,k}(S) = \frac{1}{I}\frac{G^*_k}{G^*_{LVE}}G^R \tag{2.10}$$

2.4.3 Thermodynamic-based Work Potential Theory

Researchers have used thermodynamics-based work potential theory to describe the structural changes due to loading and unloading (Schapery, 1990). This theory relates structural changes with the change in a set of internal state variables or ISVs for short. The change in this variable is associated with a change in a work potential that describes the energy released or absorbed by the material to manifest that change. According to this theory, the sum of work potentials associated with each internal state variable and the elastic strain energy density constitute the total work potential of the material. Work potential theory states that the thermodynamic force (or stress) required to bring a change in material structure via a specific damage or failure mechanism is equal to the rate of change of dissipated strain energy density with respect to the displacement (or strain) associated with corresponding damage mechanism. In a pseudo-elastic domain, the relationship of thermodynamic pseudo force or pseudo shear stress, τ^R with the pseudo strain energy in shear, W^R_s, and the pseudo shear strain, γ^R is given by (Schapery, 1990):

$$\tau^R = \frac{\partial W_s^R}{\partial \gamma^R} \tag{2.11}$$

Similarly, assuming isothermal condition, the work potential theory also expresses pseudo shear stress and pseudo shear strain energy, W_s^R as functions of the internal state variable for damage, S_s and the shear strain, γ^R (or angular displacement) associated with shear damage:

$$\tau_s^R = \tau_s^R(\gamma^R, S_s) \tag{2.12}$$

$$W_s^R = W_s^R(\gamma^R, S_s) \tag{2.13}$$

Based on these theories, the pseudo shear stress and pseudo shear strain energy responsible for the shear damage in each half of the k^{th} load cycle (see Figure 2.1) can be expressed as:

$$\tau_{oc,k}^R = IC_{s,k}^R \gamma_{oc,k}^R \tag{2.14}$$

$$W_{s,k}^R = \frac{I}{2} C_{s,k}^R \left(\gamma_{oc,k}^R\right)^2 \tag{2.15}$$

2.4.4 Rate-type Damage Evolution Law

A model based on continuum damage mechanics is used to quantify damage in terms of an internal state variable (S_s) assuming that the body under damage is a homogeneous continuum that is much larger than the flaw sizes. For time-dependent materials, Schapery (1990) proposed the rate of damage evolution as the α^{th} power function of change in pseudo strain energy in shear with respect to the internal state variable for damage, wherein the slope α refers to a material damage evolution rate parameter. Mathematically, the power law form for the damage evolution rate can be expressed as:

$$\frac{dS_s}{dt} = \left(-\frac{\partial W_s^R}{\partial S_s}\right)^\alpha \tag{2.16}$$

This function is analogous to the crack growth law in elastic materials (Paris and Erdogan, 1963) and is based on the fact that crack growth obeys a power relation in local J_v-integral (Schapery, 1984b). By using the relations from the work potential theory and applying the chain rule of derivatives, the aforementioned damage evolution law can be simplified to quantify total damage at the N^{th} cycle of shear load (Park et al., 1996):

$$S_{s,N} \approx S_{s,0} + \sum_{k=1}^{N} \Delta S_{s,k} \approx S_{s,0} + \sum_{k=1}^{N} \left[\left(-I \left(\Delta C^{R}_{s,k} \right) \left(\gamma^{R}_{oc,k} \right)^{2} \right)^{\frac{\alpha}{1+\alpha}} \left(\Delta t_{k} \right)^{\frac{1}{1+\alpha}} \right] \qquad (2.17)$$

In this expression, $S_{s,0}$ is the internal state variable for shear damage at the beginning of loading. The incremental term in the above relation signifies the total damage due to a complete load cycle (see Figure 2.1 for the pseudo shear strain energy formulation). For a specimen without any pre-existing damage, the initial damage value can be set to zero, as is the case in this study. The internal state variable for shear damage S_s starts with the lowest value (set to zero in the undamaged state) and increases with time, signifying the progressive damage growth due to shear, while the pseudo-stiffness $C^{R}_{s}(S_s)$ starts with its highest stiffness value (unity after normalization) and keeps decreasing with time. The VECD model has been widely used in describing deterioration of asphalt composites during uniaxial monotonic tests and uniaxial cyclic tests but only occasionally in cyclic shear tests. Kim et al. (2003) used modified correspondence principles and work potential theory to study damage and healing in shear mode, but only recent studies Karki et al. (2014b); Palvadi et al. (2012) utilized the damage evolution law in asphalt composites under shear. Since the damage characteristic curve is independent of the mode and amplitude of loading, it can also be used to predict the number of cycles required to degrade an asphalt material to a certain level of stiffness (or pseudo-stiffness) or to accumulate a certain degree of damage when subjected to any arbitrary loading condition. For example, the number of load cycles to reduce the stiffness ΔC and corresponding increase in damage ΔS when subjected to a strain amplitude $\gamma^{R}_{pp,k}$ is given by:

$$N \approx f \sum_{k=1}^{N} \left[\left(-I \left(\Delta C^{R}_{s,k} \right) \left(\gamma^{R}_{oc,k} \right)^{2} \right)^{-\alpha} \left(\Delta S_{s,k} \right)^{1+\alpha} \right] \qquad (2.18)$$

2.5 RESEARCH APPROACH

The focus of this research was to investigate the effect of asphalt binder oxidation and the use of RAP on the fatigue performance. To this end, fatigue-cracking characteristics of an asphalt binder were measured at different levels of aging. This research used two common aging devices to simulate aging in the laboratory: rolling thin film oven (RTFO), and pressure aging vessel (PAV). The RTFO simulates short-term aging due to construction, and the PAV simulates the long-term aging due to construction and service. Furthermore, in order to simulate extended aging, the PAV-aged asphalt binder was further aged using PAV for a second and third times. Finally to simulate a HMA containing RAP, the RTFO-aged binder was mixed with the double PAV-aged binder at two different proportions: 25 and 50 percent by mass. To measure the fatigue and fracture properties of the asphalt binder aged at different conditions, two mechanical tests were conducted: glass bead standardized composite and thin film fracture tests. The test methods proposed here were based on the recognition that the stress state of the asphalt binder within the mixture has a significant influence on the mode of failure. The test results were analyzed using viscoelastic continuum damage (VECD) mechanics. This analysis method is robust and allows comparing the fatigue test results conducted at different loading condition.

CHAPTER 3. MATERIALS

3.1 MATERIAL SELECTION AND PREPARATION

An asphalt binder with performance grade of PG 67-27, following the Superpave performance grading system, was selected for this study. To investigate the effect of aging on the fatigue and fracture performance of asphaltic materials, this binder was aged to different levels in the laboratory. First, a rolling thin film oven (RTFO) was used to simulate short-term aging that occurs during mixture production and placement. Then, a pressure-aging vessel (PAV) was used to simulate the long-term aging due to weathering and oxidation. The RTFO aging was carried as per ASTM D2872, where 35 grams of the binder was poured into the RTFO bottles, and aged in the RTFO for 85 minutes. The RTFO aged binder residues were further aged in the PAV to simulate long-term aging of the binders. The PAV aging process was carried out as per ASTM D6521, where 50 grams of the RTFO residue was poured into the PAV pans and aged in the PAV for 20 hours at the temperature of 100°C (212°F). In order to investigate the effect of extended aging the residue recovered from the PAV was further aged using PAV for a second and third times. Figure 3.1 shows the aging procedure and stages used in this study.

Furthermore, one of the objectives of this study was also to investigate the effect of the use of reclaimed asphalt on the fatigue and fracture properties of asphaltic materials. For this purpose, the PAV2 aged binder representing the reclaimed binder was mixed with RTFO aged binder representing the new binder in construction that experienced short-term aging due to construction. Also the simulated reclaimed asphalt (PAV2 aged binder) was mixed with RTFO aged binder at two different dosages: 25 and 50 percent. To investigate the effect of aging on the fracture and fatigue properties of asphaltic materials, this research will used two different test methods: thin film fracture test and fatigue test using a standardized composite including glass beads of different sizes and asphalt binder. The following two sections describe the sample preparation for these test methods.

3.2 SPECIMEN FABRICATION FOR STANDARDIZED COMPOSITE TEST

Standardized composite test geometry is composed of asphalt binder and glass beads of different sizes. Three different sizes of the glass beads were used to create a gradation that closely followed the maximum density line on a 0.5 power chart (Figure 3.2). Figure 3.2

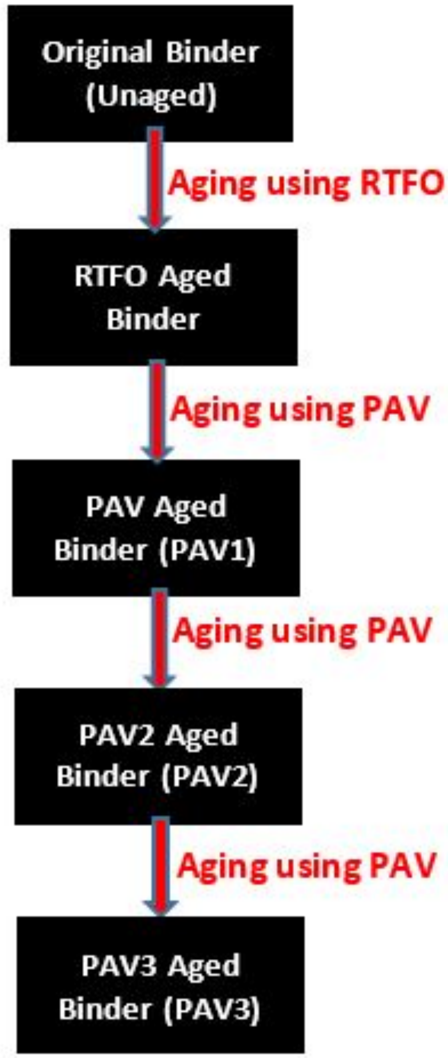

Figure 3.1. Aging procedure and stages used in this study.

illustrates the size and proportion of each glass bead size. The optimal binder content was determined by trial and error. Mixes were prepared and compacted using several different binder contents. A preliminary study conducted by the authors showed that the specimens prepared using 10% binder by weight of the glass beads would be optimal. Compacted specimens with low asphalt binder contents were found to be too brittle and susceptible to breakage during handling and specimen preparation. On the other hand, specimens with high asphalt binder contents were found to have problems related to flushing and deformation. A more thorough investigation of the binder content and its influence on the stress-state when used as a matrix with glass beads as an inclusion was beyond the scope of this study and will be investigated in our future work.

Figure 3.2. Gradation of glass beads used to produce specimens for standardized composite test

To prepare the asphalt binder-glass bead mixture, the following procedure was used. The asphalt binder was heated to 150°C in a 100 g can enclosed in a temperature controlled jacket. A thermocouple was used to constantly monitor the temperature of the binder throughout the process. The appropriate amount of glass beads were weighed in advance and oven dried. Once the binder reached the target temperature, the glass beads were slowly added to the binder while constantly stirring the mix in the temperature jacket. The mixing was done by adding glass beads of each size at a time, starting from the smallest to the largest size (0.1 mm, 0.5 mm and 1 mm). The beads and the asphalt binder were thoroughly mixed manually until a homogenous mix was obtained. Figure 3.3 illustrates the mixing of the glass beads with the asphalt binder.

After mixing, the contents were transferred to a stainless steel mold to compact and fabricate test specimens. A two-piece stainless steel mold was fabricated to compact and prepare the test specimens. The mold had a total height of 75 mm and internal diameter of 12.5 mm. The mold also had a stop at the bottom and the compaction rod at the top was designed to allow dropping a fixed weight of 335 g from a fixed height of 75 mm. The two pieces of the mold were held together using two pipe clamps. Figure 3.4 shows the

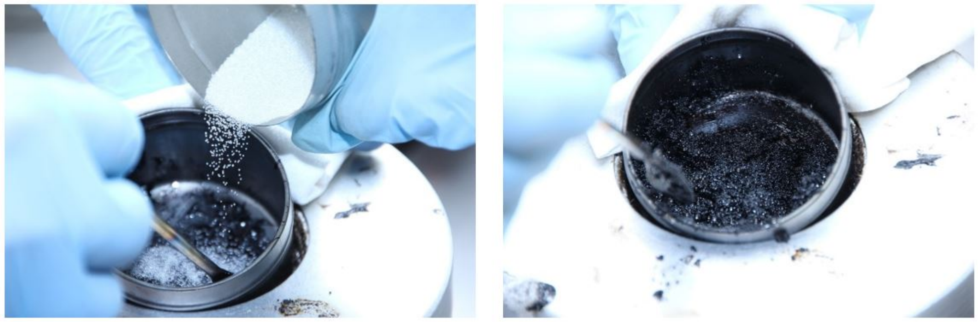

Figure 3.3. Manually mixing glass beads with the asphalt binder to prepare a homogenous mixture

manufactured mold and its components. A total of three molds were fabricated to be able to fabricate three test specimens using the loose mix at the same time and minimize the amount of variability and reheating required.

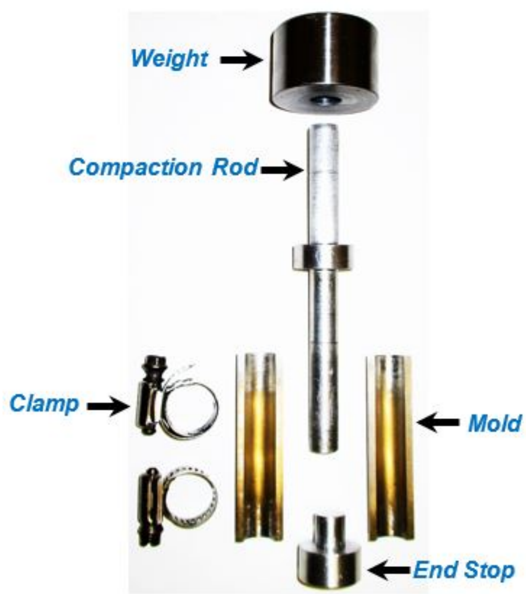

Figure 3.4. Manufactured mold assembly for compaction

In order to prepare the molds for compaction, first the compaction rod and inside of the stainless steel molds and were lubricated using a silicon lube spray. Then, the assembled molds and compaction rod were heated to 150°C in a convection oven. The silicon spray was used to ease removal of the sample from the mold. When the loose mix became ready, the molds were removed from the oven one at a time. The loose mix was poured in the mold about two-thirds of the way full. The loose mix was then compacted using the compaction rod and dropping the weight from the fixed height for 25 times. Figure 3.5 illustrates these two steps.

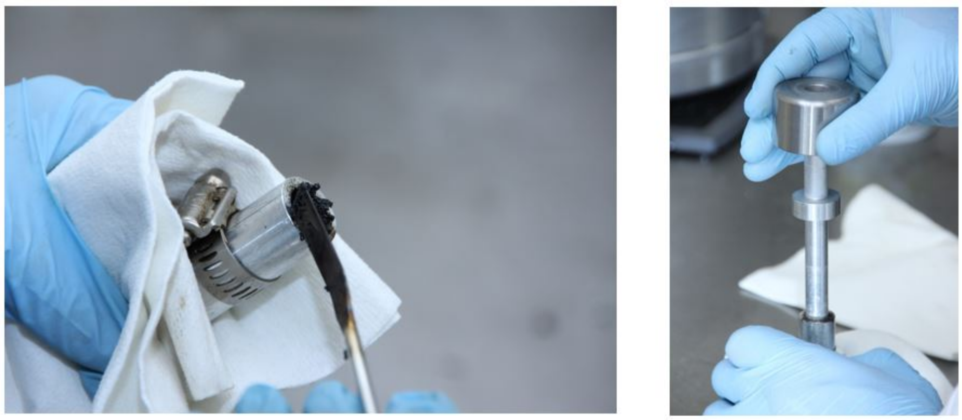

Figure 3.5. Glass bead mixture being poured into the mold and compacted using the rod and drop weight

It should be noted that the previous study by the authors (Motamed et al., 2013) on a similar test geometry revealed that compacting the specimen in two or three layers resulted in weak interfaces. This resulted in the failure of the test specimens along a horizontal planes associated with these weak interfaces. Therefore, the authors decided to compact the specimens in a single layer. Furthermore, the authors conducted several trials to determine the number of drops required to compact the specimen. Based on these trials it was determined that the specimen height did not change after 25 drops. After compaction, the specimens were allowed to cool down to the room temperature in the molds for 24 hours. After this time the clamps holding the two piece mold were removed. Then, the bottom of the mold was removed and the two halves of cylindrical mold were gently opened to extract the specimen. In some cases the specimens remained adhered to the mold. In such cases, the surface of the mold was gently warmed to facilitate the separation. Once the test specimen was obtained from the mold, the ends of the specimen were glued to metal end caps using high strength epoxy. Allowing the high strength epoxy to set completely, the test specimen was mounted onto a DSR for fatigue testing in shear. Figure 3.6 shows the test specimen and the tests setup in DSR. A total of six specimens were fabricated and tested for each of the aging conditions.

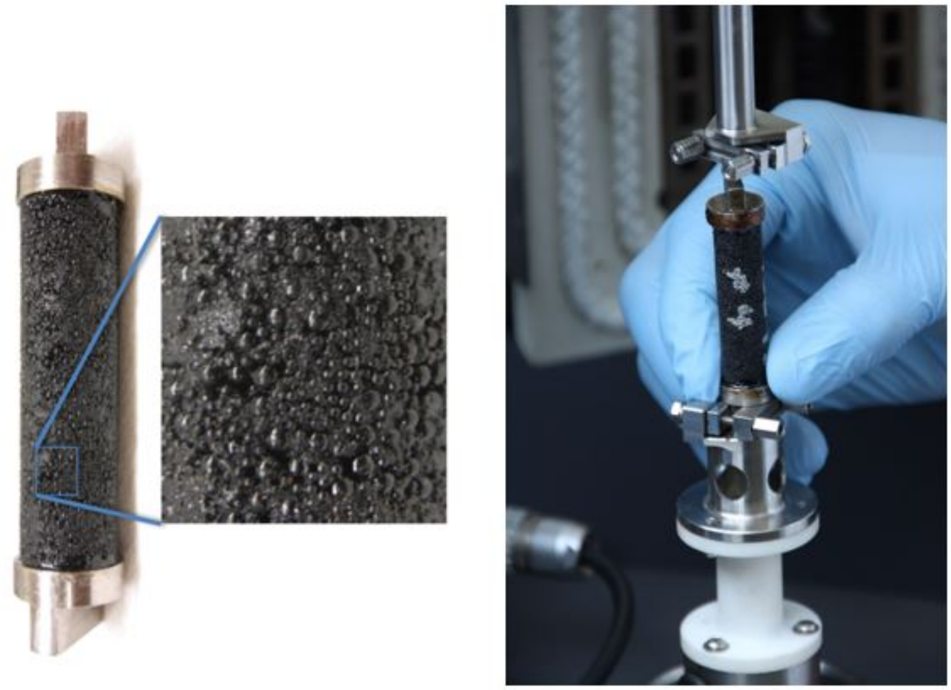

Figure 3.6. A test specimen and the test setup in Dynamic Shear Rheometer

3.3 SPECIMEN FABRICATION FOR THIN FILM FRACTURE TEST

To conduct thin film fracture tests, a circular poker-chip test geometry was used. Circular poker-chip test geometry is disc-shaped specimens between two circular metal specimen holders. Circular shape specimen were used to reduce singular corners. Metal discs were manufactured with diameter of 14.6 mm. Poker-chip test specimens with the height of roughly 300 micrometer were fabricated using the following procedure. First the end plates were clamped to the tension-compression dynamic mechanical analyzer DMA, and the device was conditioned for a duration of one hour at the testing temperature. After the instrument reached steady state, the zero gap was established. Then the asphalt binder was placed on the lower metal plate and the temperature was raised to 100°C. Raising the temperature to 100°C had several advantages:

- it allowed the asphalt binder to spread uniformly,
- it released any trapped air bubbles in the asphalt binder,
- it promoted bonding between the binder and the metal plates,

- it minimized the effect of physical hardening on the test results.

After holding the temperature at 100°C for 5 minutes, the temperature was decreased to 60°C, which seems to be an appropriate temperature for squeezing asphalt binders. Finally, thin films with the height of roughly 300 micrometer were prepared by lowering the upper plate and squeezing the asphalt binder between two metal end plates. To avoid any thermal stresses in specimens, first the upper plate was approximately lowered to a gap of 320 micrometer. Then, as the temperature was lowered to the testing temperature, the material and system were allowed to shrink by maintaining zero normal force in the specimen. It took almost forty minutes to reach the thermal and concomitant shrinkage equilibrium. Therefore, specimens were conditioned for one hour at the testing temperature before trimming the edge of the specimen. Trimming was followed by another hour of conditioning before the displacement controlled test began. Figure 3.7 illustrates the thin film fracture test set-up.

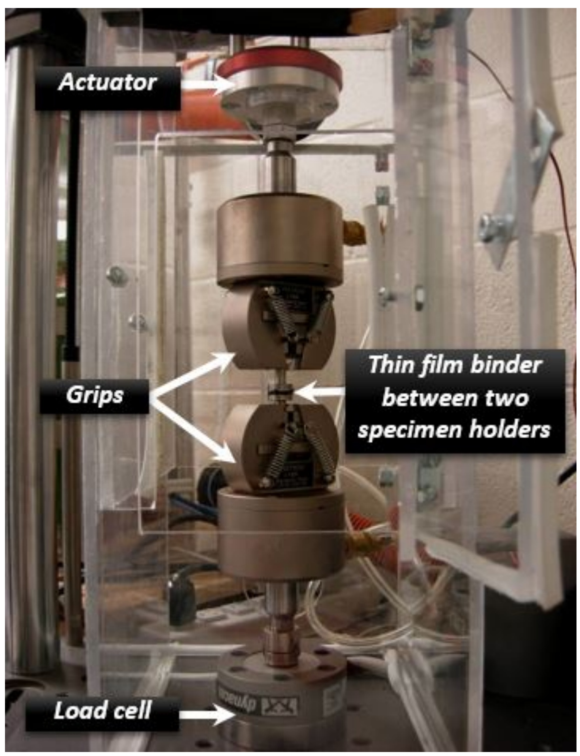

Figure 3.7. Thin film fracture test set-up

CHAPTER 4. TEST METHODS, ANALYSIS AND RESULTS

This research investigates the effect of aging on the fracture and fatigue properties of asphaltic materials. To this end, the authors used two different test methods: thin film fracture test and fatigue test using a standardized composite. The following two subsections describe the test methods used in this study and the analyses conducted.

4.1 STANDARDIZED COMPOSITE TEST

A Dynamic Shear Rheometer DSR (Model TA AR2000Ex) was used to measure the mechanical response of the glass bead composites when subjected to different shear stress levels. The two main objectives of the tests conducted using the DSR were to obtain the linear viscoelastic and fatigue properties of the glass bead specimens subjected to torsion. The following are some more details pertaining to the tests conducted using a DSR. All tests described in this section were conducted at an intermediate temperature of 20°C. The test specimens were mounted in the DSR and were conditioned at the test temperature for at least 1 hour to ensure that they reached thermal equilibrium.

4.1.1 Linear viscoelastic properties

All test specimens were subjected to a creep-recovery test as well as a cyclic test to obtain the linear viscoelastic properties at 20°C. The following sequence of loads was used to obtain the linear viscoelastic properties. First, a set of creep and recovery tests at different stress levels were conducted to ensure that standardized composites behaved linearly in the stress levels used for this test. The creep part of the test was three seconds long. This loading time was long enough to collect the time dependent response of material for the time window of interest. The selected loading time was much greater than the rise time of the instrument, which is on the order of 10^{-4} seconds. This minimized the transient effects on the measured data. On the other hand, the loading time was not too long to risk damaging the material. The recovery time of 200 seconds was considered long enough to achieve significant if not complete recovery. Three different stress levels were selected to obtain the material response: 5 kPa, 10 kPa, and 20 kPa. Creep and recovery at each stress level were repeated twice before proceeding to the next stress. Results from the second repeat were compared to the first repeat in order to detect any permanent change or damage to the material during the loading period. Figure 4.1 shows the creep and recovery test results for PAV3 aged binder at two different stress levels (the third stress level is not shown for clarity). Using the measured strains $\gamma(t)$ under constant shear stress τ_0 , the creep compliance $J(t)$ was calculated at different stress levels:

$$J(t) = \frac{\gamma(t)}{\tau_0} \tag{4.1}$$

Figure 4.2 shows the measured creep compliance for the PAV3 aged binder at three different stress levels. As can be seen, the creep compliance at different stress levels remains the same and does not change with stress level. This indicates that material is behaving linearly at these stress levels and there is no damage or change in materials due to loading.

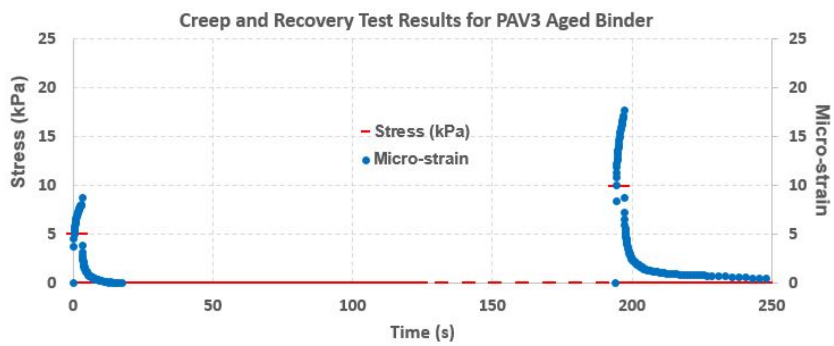

Figure 4.1. Creep and recovery test results for PAV3 aged binder under 5 and 10 kPa stress levels

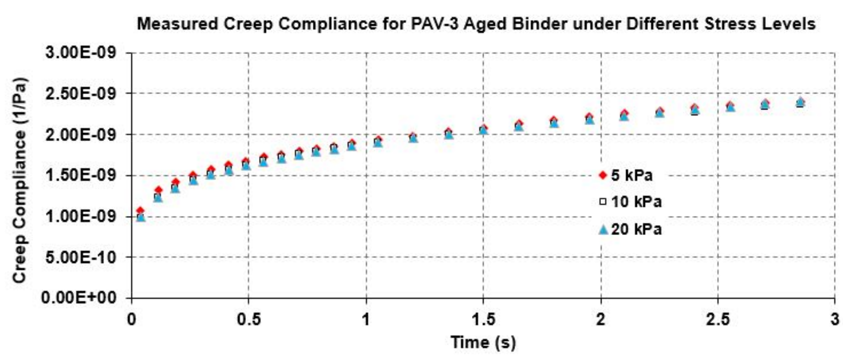

Figure 4.2. Measured creep compliance for PAV-3 aged binder under different stress levels at 20°C

Furthermore, it was observed by the authors that a power-law form for the compliance fits well to the measured creep and recovery data:

$$J(t) = J_0 + J_1 t^m \tag{4.2}$$

where J_0, J_1, and m are material constants; and t is the time in seconds. Due to higher sensitivity of these constants to the test duration in creep, these material constants were obtained using only the recovery test data (Hiel et al., 1984). Figure 4.3 compares the measured creep response of PAV3 aged binder with the estimated creep response for a stress level of 5 kPa. The material response was estimated using Boltzmann Integral and the power law equation calibrated using the recovery data. As can be observed, the power law equation is adequate to model the linear behavior of the composite.

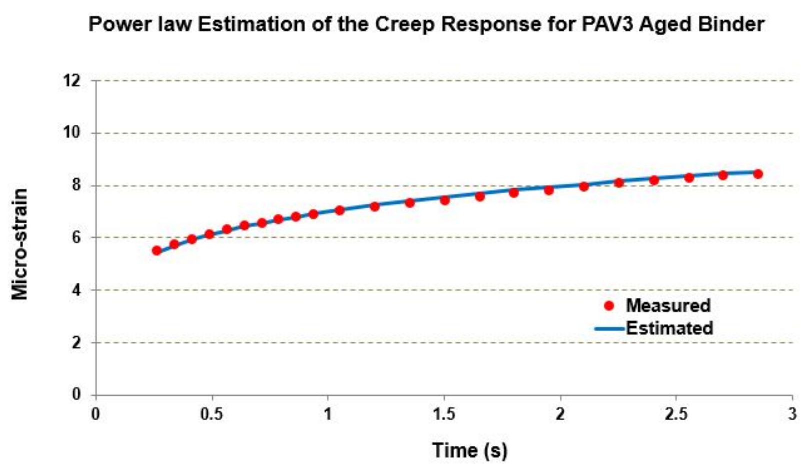

Figure 4.3. Power law estimation of the creep response for PAV3 aged binder under a constant load of 5 kPa at 20°C

Figures 4.4 and 4.5 compares the J_1 and m values for the different mixes used in this study. The values of these two parameters indicate how much a material's response is time-dependent. As can be observed, both m value and J_1 reduced with aging. This indicates that as the material goes through aging, it becomes more stiff and less time dependent. Engineers typically regard an increase in stiffness and reduced ability to relax as the reasons for crack nucleation and fatigue failure. After creep and recovery, to obtain the linear viscoelastic properties of standardized composites in frequency domain, the test specimen was subjected to a sinusoidal load with a frequency of 10 Hz and stress amplitudes of 10 and 20 kPa. The complex modulus and phase angle were recorded only using the last few cycles at each stress level to minimize the influence of the initial transients. It should be noted that although the complex modulus for the complete frequency spectra can be calculated using the principle of superposition with the data from the creep-recovery curve, this test was conducted to provide a more robust estimation of the linear viscoelastic properties. Figures 4.6 and 4.7 compare the linear dynamic shear modulus G^* and phase angle δ of the asphalt binder at different levels of aging. The test results in frequency domain also demonstrate that oxidative aging makes the asphaltic materials more stiff (increase in dynamic shear modulus) and less time dependent (decrease in phase angle).

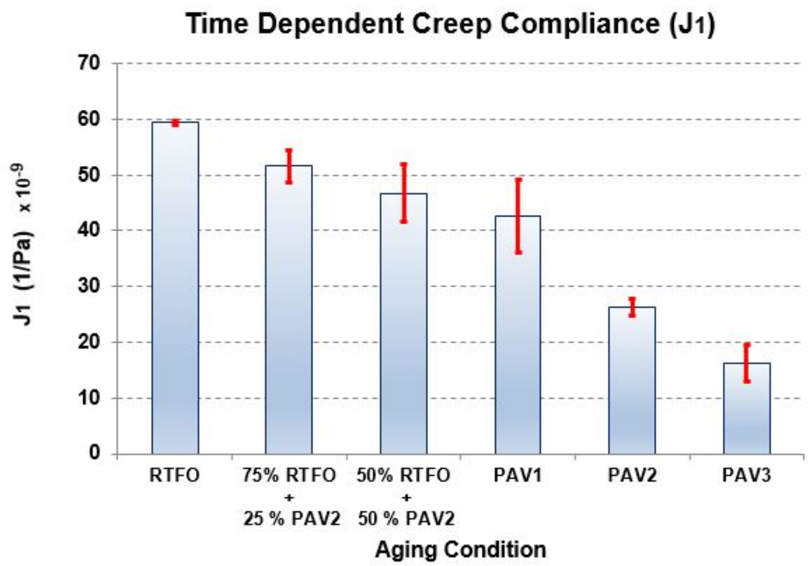

Figure 4.4. Coefficient of the time-dependent term in the power law equation or J_1 for different levels of aging at 20°C

As discussed in the previous section, current standard for characterizing asphalt binder considers the $G^*Sin\delta$ as an indicator of the asphalt binders' resistance to fatigue cracking. Not withstanding, that this parameter is intended for use with asphalt binders, it was also calculated for the standardized composite specimens used in this study. Figure 4.8 compares the $G^*Sin\delta$ parameter for different levels of aging. The observation that can be made from these results is that the $G^*Sin\delta$ parameter was similar for different levels of aging of tested asphalt binder. This suggests that although the dynamic modulus increases with oxidization, the viscous component of the dynamic modulus $(G'' = G^*Sin\delta)$ remains approximately unchanged. As discussed previously, either the creep compliance (time domain) or the complex modulus from cyclic tests (frequency domain) can be used to estimate the linear viscoelastic properties of the test specimens. In this case, we conducted both tests to ensure the robustness of the linear viscoelastic properties that will be subsequently used

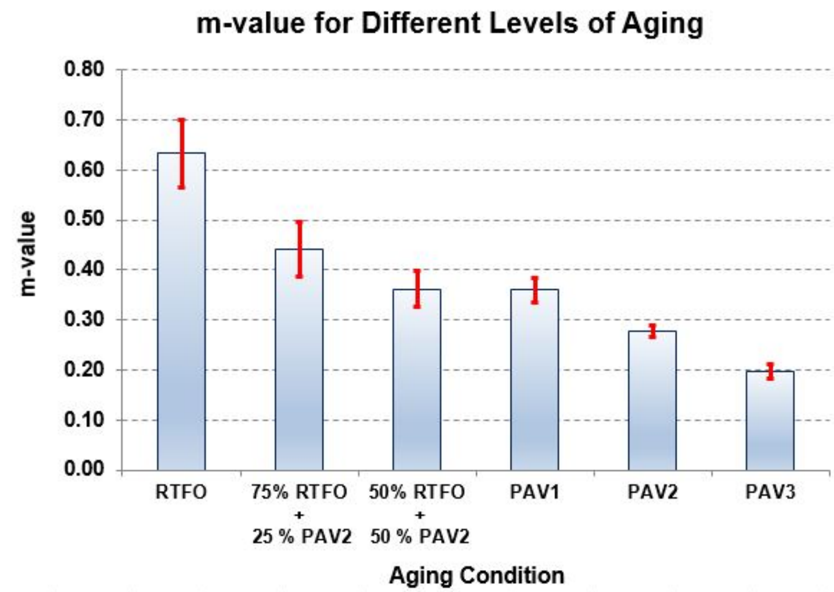

Figure 4.5. The exponent in the power law equation or m-value for different levels of aging at 20°C

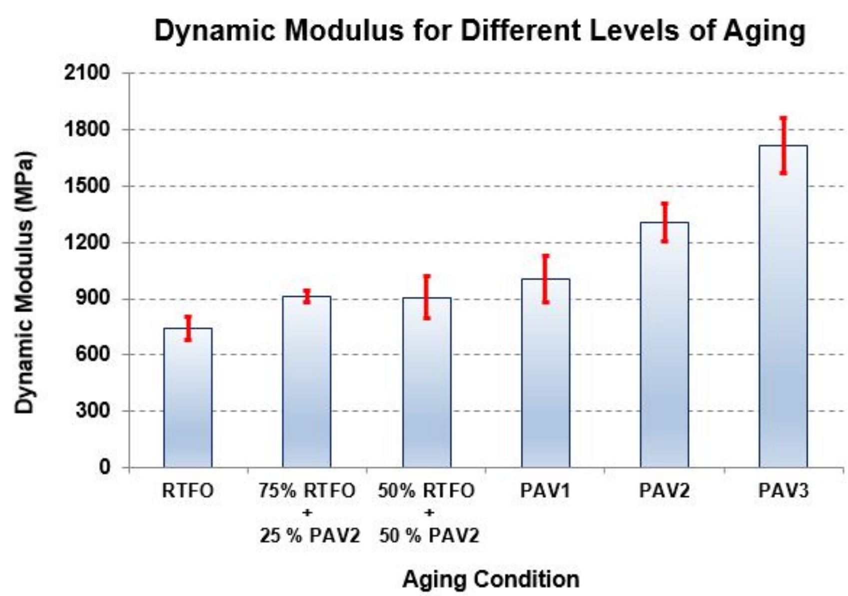

Figure 4.6. Linear viscoelastic dynamic shear modulus for different levels of aging at 10Hz and 20°C

for damage analysis.

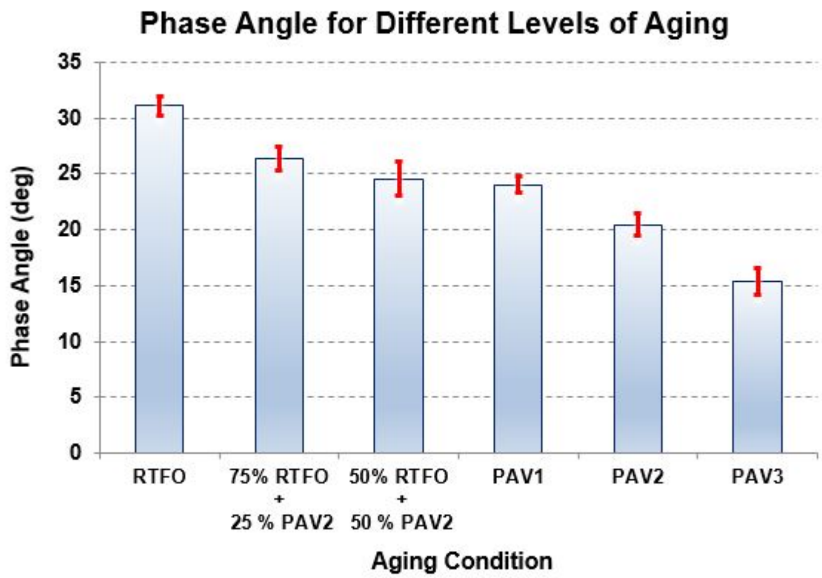

Figure 4.7. Linear viscoelastic phase angle for different levels of aging at 10Hz and 20°C

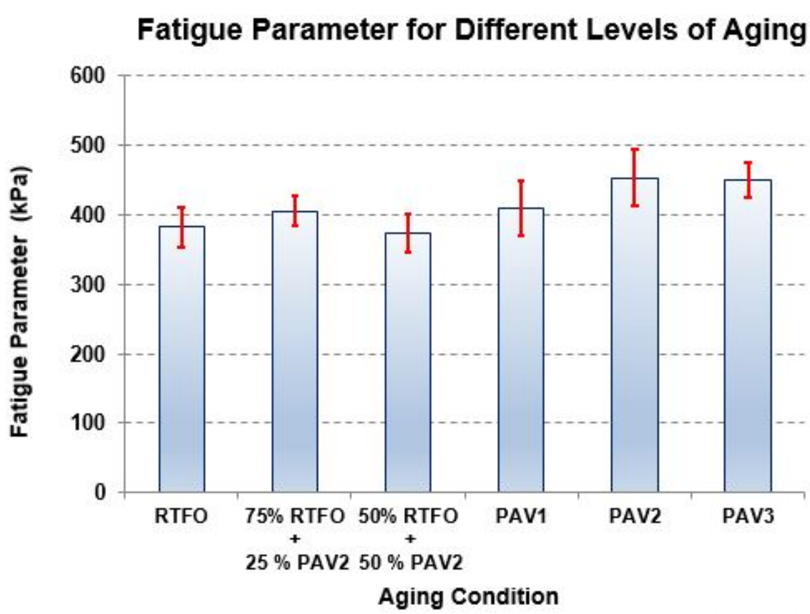

Figure 4.8. Fatigue parameter ($G^{*}Sin\delta$) for different levels of aging at 20°C

4.1.2 Fatigue behavior

To evaluate the fatigue cracking resistance of the asphalt binder at different levels of aging, cyclic tests at different stress levels were conducted. The frequency of all these tests was

10 Hz and testing temperature was 20°C. The stress amplitude ranged from 180 to 330 kPa. The reason for using different stress amplitudes was to collect an appropriate amount of data in an acceptable amount of time. Using a high stress level will result in specimen failure in the first few cycles. On the other hand, using a low stress level can lead to testing times that are not practical. The termination criteria for fatigue test were either the stiffness reaching 50 % of the initial dynamic modulus (the modulus at the beginning of the fatigue test) or the maximum of 40 hours. Figure 4.9 illustrates typical fatigue test results for PAV3 aged asphalt binder at 330 kPa stress level.

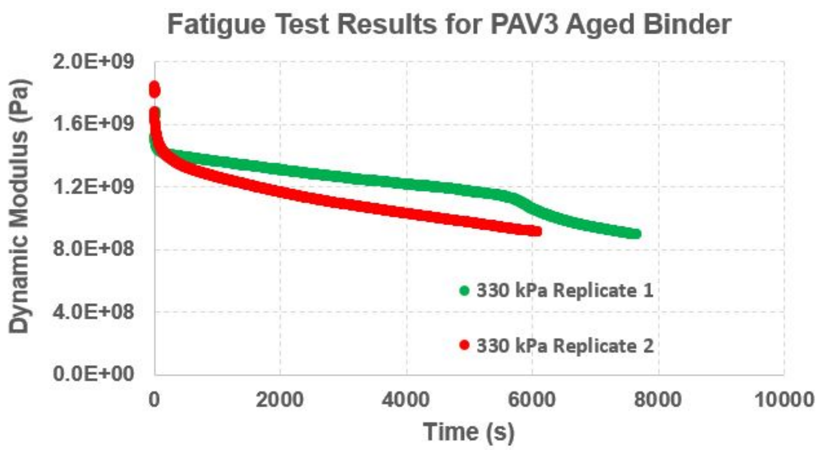

Figure 4.9. Fatigue test results for PAV3 aged binder at 330 kPa, 20°C, and 10 Hz

In order to compare the fatigue test results for the asphalt binder at different levels of aging under the same loading condition, the VECD method to evaluate damage was employed. Using this approach (Equation 2.17), the damage characteristic curve for each aging condition was obtained. Figure 4.10 demonstrates a typical damage evolution curve (C vs S) obtained for PAV3 aged binder.

Then, the authors used the damage evolution curves of the material at different levels of aging and Equation 2.18 to calculate and compare the fatigue life of these materials under a reference loading condition. The reference loading condition was considered to be the lowest stress level used in this study for fatigue testing, i.e, 180 kPa. Figure 4.11 compares the fatigue life of the binder material at different levels of aging. It should be noted here that the fatigue life is the number of loading cycles required to reach to 50% of initial modulus. As can be seen, aging has resulted in improved fatigue performance of the asphalt binder. However, this observation requires further investigation using different modes of loading and testing conditions.

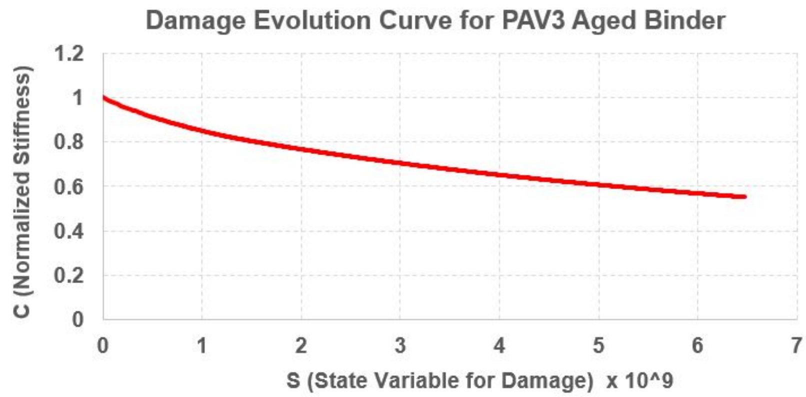

Figure 4.10. Typical damage evolution curve (C vs S) obtained for PAV3 aged binder

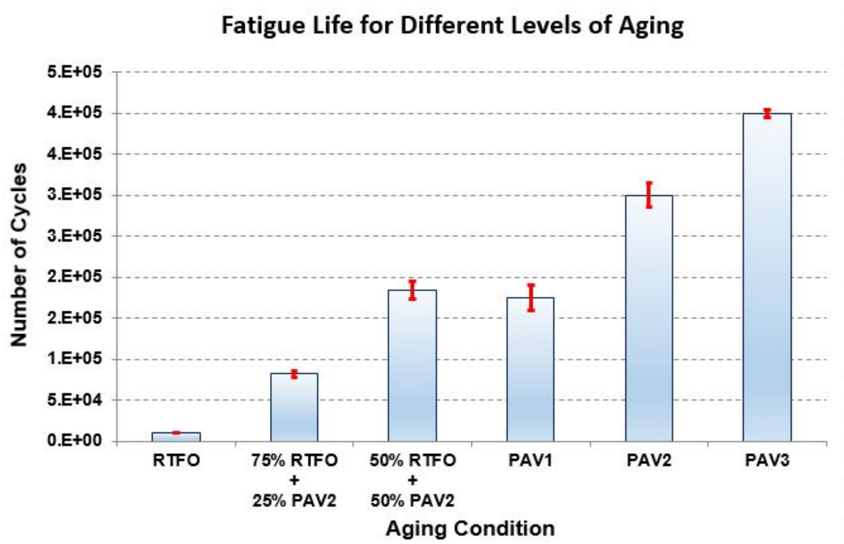

Figure 4.11. Fatigue life (cycles required for reaching to 50% of initial modulus) for different levels of aging

4.2 THIN FILM FRACTURE TEST

The thin film fracture test was conducted to measure the fracture properties of the asphalt binder at different levels of aging. In order to conduct the fracture test, a tension-compression dynamic mechanical analyzer (DMA- Model Instron ElectroPuls E1000) was used. These tests were also conducted at an intermediate temperature of 20°C, similar to the standardized composite test. To ensure the same testing temperature inside the testing device, dummy specimens with a thermocouple in the middle were used for calibration of the temperature controller. As described earlier, the test specimens were fabricated in the DMA and were conditioned at the test temperature for at least 1 hour to ensure that the test specimens reached thermal equilibrium. All the fracture tests were conducted by applying a displacement-controlled monotonic loading with the rate of 1 micrometer/sec. Measuring the applied displacement and generated force during the test, the authors calculated the nominal stress and strain experienced by specimens. Figure 4.12 illustrates the typical test results from the monotonic fracture test on PAV aged binder for three replicates. Figure 4.13 compares the fractures properties of tested asphalt binder at different level of aging. Note that this figure illustrates the average response for three to four replicates with the exception of the PAV3 binder. The two replicates for the PAV3 binder are illustrated to demonstrate the high variability and different modes of failure that were experienced with this particular binder.

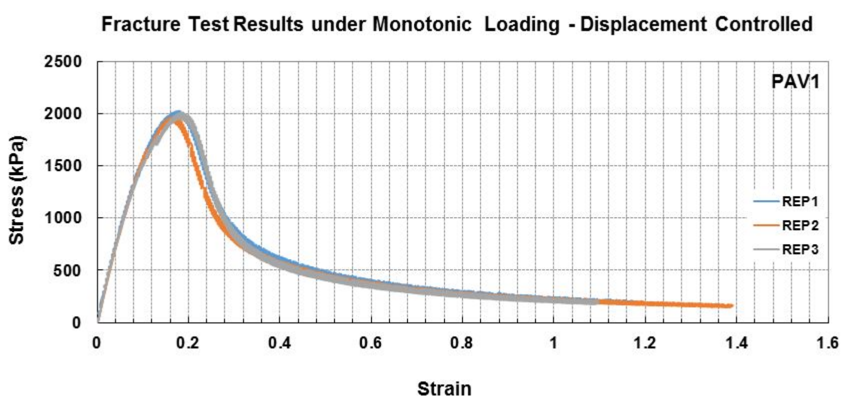

Figure 4.12. Monotonic fracture test results for PAV aged binder at the rate of 1micrometer/second

Using these results, maximum tensile stress and fracture energy of the asphalt binders were calculated. The fracture energy was calculated as the area under the stress-strain curve for the strain ranging from zero (start of the test) to the strain at which the yielding occurs (peak load). Figures 4.14 and 4.15 summarize and compare the maximum tensile stress and the fracture energy of the tested asphalt binder at different levels of aging. As can be seen, both maximum tensile stress and fracture energy increase until some level of aging. Aging beyond the level identified as PAV1 does not improve these parameters. A similar trend was observed for the strain at which yielding (maximum tensile stress) occurs (Figure 4.13). In contrast, the strain at which the physical separation of specimens occur continuously decreases with aging. The fracture and fatigue test results obtained for

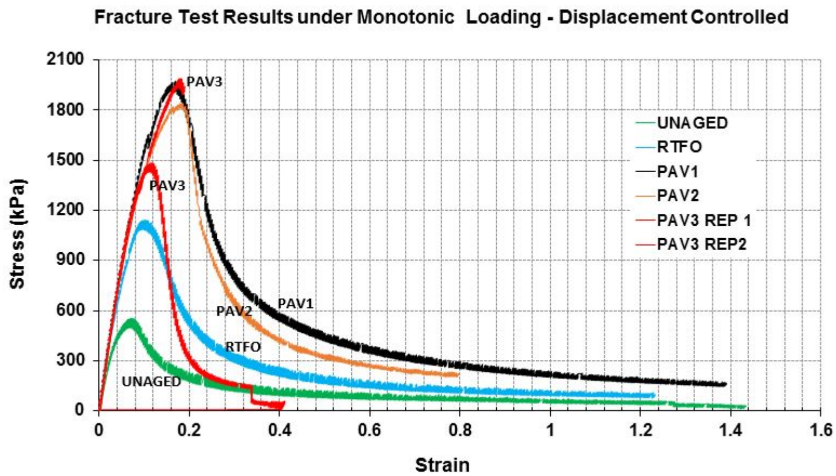

Figure 4.13. Comparison of the fracture behavior of the tested asphalt binder at different levels of aging

mixtures that simulate RAP mixes demonstrated that the performance of these mixtures are somewhere in between that of their components.

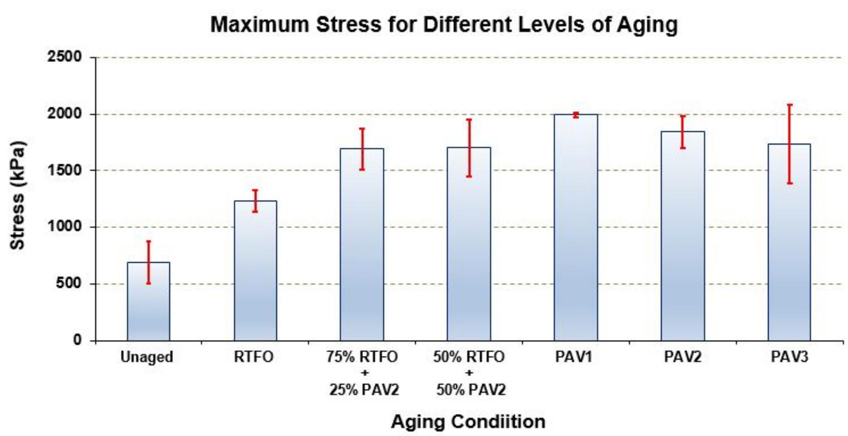

Figure 4.14. Comparison of the maximum tensile stress for different levels of binder aging

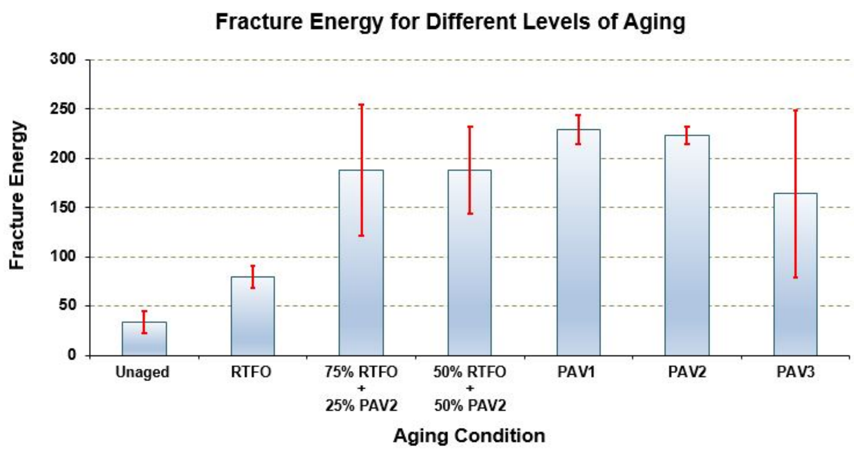

Figure 4.15. Comparison of the fracture energy for different levels of binder aging

CHAPTER 5. SUMMARY OF FINDINGS

This study investigated the effect of asphalt binder oxidation on its fracture properties and fatigue cracking performance. To this end, fatigue cracking resistance and fracture properties of a selected asphalt binder were measured at different levels of aging. The fatigue test was conducted using a standardized glass bead composite under cyclic load, and the fracture test was conducted using a poker chip test geometry under monotonic loading.

The following are some of the main findings from this study:

1. Creep - recovery and cyclic loads were used at low stress levels in shear to determine the linear viscoelastic properties of glass bead composites at different levels of aging. As expected, the results showed that aging causes the asphalt binder and concomitant composite to become more stiff and relatively less time dependent.

2. Cyclic loads were applied at low stress levels in shear with the glass bead composite to compute the fatigue parameter introduced by SHRP for asphalt binder, i.e., $G^{*}Sin\delta$, which also represents the loss modulus or viscous component of the asphalt binder. As evidenced by Figure 4.8, the viscous component of dynamic modulus does not change significantly with aging.

3. The results from fatigue test using glass bead composite subjected to stress controlled cyclic load, clearly demonstrated that the fatigue cracking resistance of asphalt binder increased with aging.

4. The results from thin film fracture test illustrate that both maximum tensile stress and fracture energy increase until some level of aging. Aging beyond PAV1 did not significantly improve these parameters. Interestingly, a similar trend was observed for the strain at which yielding (maximum tensile stress) occurs. However, as can be clearly seen in Figure 4.13, the strain at which the physical separation of specimens occur continuously decreases with aging.

This study also investigated the effect of using reclaimed asphalt pavement on the mechanical properties and performance of newly constructed roads. To simulate the binder in a HMA containing RAP, the RTFO-aged (short-term aged) binder was mixed with the double PAV-aged (long-term aged) binder in two different percentages. The amount of RAP used herein represented the typical percentage use of RAP. The results demonstrate that the mechanical properties and performance of the mix containing RAP reflect a composite effect of its components. In summary, the findings from this work suggest that although aged binder and concomitant RAP mixes may have higher stiffness due to aging, these materials also tend to show an increased fracture and fatigue cracking resistance. Consequently, both of these factors must be considered in order to fully optimize mix designs containing RAP and maximize the use of these materials.

The scope of this study was limited and only one binder was used. It is recommended for future work that these findings be further verified using different asphalt binders at different aging and loading conditions. The authors recognize that the fatigue cracking resistance was compared at similar levels of stress. In the context of traffic loading, it can be argued that the pavement structure is always subjected to a certain level of stress (and not deformation) that corresponds to the vehicle load and tire configuration. However, in the context of thermal loads, the pavement structure experiences a certain level of strain that corresponds to the temperature and coefficient of thermal expansion of the material. This study only focused on the former and concluded that the aged binders typically had better fatigue and fracture resistance at when subjected to similar levels of stress. It is equally important that future studies extend this work to thermal fatigue and in-particular to the performance of aged binders at low temperatures. However, for such future studies, it must be recognized that both stiffness and strength of the material are important in dictating the material performance.

REFERENCES

Anderson, D., Hir, Y., Marasteanu, M., Planche, J.-P., Martin, D., and Gauthier, G. 2001. Evaluation of Fatigue Criteria for Asphalt Binders. *Transportation Research Record: Journal of the Transportation Research Board*, 1766:48–56.

Andriescu, A. and Hesp, S. A. 2009. Time-temperature superposition in rheology and ductile failure of asphalt binders. *International Journal of Pavement Engineering*, 10(4):229–240.

Arega, Z., Bhasin, A., Motamed, A., and Turner, F. 2011. Influence of warm-mix additives and reduced aging on the rheology of asphalt binders with different natural wax contents. *Journal of Materials in Civil Engineering (ASCE)*, 23(10):1453–1459.

Bahia, H. U., Wen, H., and John, C. 2010. Developments in intermediate temperature binder fatigue specifications. Transportation Research Circular, pages 25–33. Transportation Research Board, Washington, D.C.

Daniel, J. S. 2001. *Development of a Simplified Fatigue Test and Analysis Procedure Using a Viscoelastic, Continuum Damage Model, and its Implementation to Westrack Mixtures*. PhD thesis.

Daniel, J. S. and Kim, Y. R. 2002. Development of a Simplified Fatigue Test and Analysis Procedure Using a Viscoelastic, Continuum Damage Model. *Journal of the Association of Asphalt Paving Technologist*, 71.

Decker, D. S. 1997. State-of-the practices for use of RAP in hot mix asphalt. *Journal of the Association of Asphalt Paving Technologists*, 66:704.

Ferry, J. D. 1980. *Viscoelastic Properties of Polymers*. Wiley.

Graham, G. A. C. and Sabin, G. C. W. 1973. The correspondence principle of linear viscoelasticity for problems that involve time-dependent regions. *International Journal of Engineering Science*, 11(1):123–140.

Hiel, C., Cardon, A. H., and Brinson, H. F. 1984. Viscoelastic modelling of epoxy-resins for adhesive and composite applications. In *5th International Congress on Experimental Mechanics*, pages 263–266, Montreal, Canada.

Johnson, C. 2010. *Estimating asphalt binder fatigue resistance using an acceleratetd test method*. PhD thesis, Madison, WI.

Karki, P., Bhasin, A., and Little, D. N. 2014a. Experimental method to quantify overall damage and healing in asphalt composites using continuum damage approach. In *93rd Annual Meeting, Transportation Research Board*, Washington, D.C.

Karki, P., Li, R., and Bhasin, A. 2014b. Quantifying overall damage and healing behavior of asphalt materials using continuum damage approach. *International Journal of Pavement Engineering*, In Review.

Karlsson, R. and Isacsson, U. 2006. Material-Related Aspects of Asphalt Recycling. State-of-the-Art. *Journal of Materials in Civil Engineering*, 18(1):81–92.

Kim, Y., Lee, H. J., Little, D. N., and Kim, Y. R. 2006. A Simple Testing Method to Evaluate Fatigue Fracture and Damage Performance of Asphalt Mixtures (With Discussion). *Journal of the Association of Asphalt Paving Technologists*, 75.

Kim, Y. R. and Little, D. N. 1990. One-Dimensional Constitutuve Modeling of Asphalt Concrete. *Journal of engineering mechanics*, 116(4):751–772.

Kim, Y. R., Little, D. N., and Lytton, R. L. 2003. Fatigue and Healing Characterization of Asphalt Mixes. *Journal of Materials in Civil Engineering (ASCE)*, 15(1):75–83.

Lee, H.-J. and Kim, Y. R. 1998. Viscoelastic Constitutive Model for Asphalt Concrete under Cyclic Loading. *Journal of engineering mechanics*, 124(1):32–40.

Motamed, A., Bhasin, A., and Izadi, A. 2013. Evaluating fatigue cracking resistance of asphalt binders in a standardized composite using continuum damage theory. *Journal of Materials in Civil Engineering (ASCE)*, 25(9):1209–1219.

Olard, F. and Di Benedetto, H. 2004. Fracture toughness and fracture energy of bituminous binders at low temperatures. pages 359–366, Limoges, France.

Palvadi, S., Bhasin*, A., and Little, D. N. 2012. Method to quantify healing in asphalt composites by continuum damage approach. *Transportation Research Record: Journal of the Transportation Research Board*, 2296(1):86–96.

Paris, P. and Erdogan, F. 1963. A critical analysis of crack propagation laws. *Journal Of Basic Engineering*, 85:528–534.

Park, S. W., Richard Kim, Y., and Schapery, R. A. 1996. A viscoelastic continuum damage model and its application to uniaxial behavior of asphalt concrete. *Mechanics of Materials*, 24(4):241–255.

Park, S. W. and Schapery, R. A. 1997. A Viscoelastic Constitutive Model for Particulate Composites with Growing Damage. *International Journal of Solids and Structures*, 34(8):931–947.

Planche, J.-P., Anderson, D. A., Gauthier, G., Le Hir, Y. M., and Martin, D. 2004. Evaluation of fatigue properties of bituminous binders. *Materials and Structures*, 37:356–359.

Roberts, F. L., Kandhal, P. S., Brown, E. R., Lee, D. Y., and Kennedy, T. W. 1996. *Hot Mix Asphalt Materials, Mixture, Desgin, and Construction*. National Asphalt Pavement Association Research and Education Foundation, Lanham, Maryland.

Schapery, R. A. 1984a. Correspondence principles and a generaiized J integral for large deformation and fracture analysis of viscoelastic media. *International Journal of Fracture*, 25:195–223.

Schapery, R. A. 1984b. Correspondence Principles and a Generalized J Integral for Large Deformation and Fracture Analysis of Viscoelastic Media. *International Journal of Fracture*, 25(3):195–223.

Schapery, R. A. 1989. On the Mechanics of Crack Closing and Bonding in Linear Viscoelastic Media. *International Journal of Fracture*, 39:163–189.

Schapery, R. A. 1990. *Characterization of Viscoelastic Materials*.

Tschoegl, N. W. 1989. *The Phenomenological Theory of Linear Viscoelastic Behavior*. Springer-Verlag, New York.

Tyrion, F. C. 2000. Asphalt Oxidation. Asphaltenes and Asphalts. *Developments in Petroleum Science*, 40B.

Underwood, B. S., Kim, Y. R., and Guddati, M. N. 2010. Improved calculation method of damage parameter in viscoelastic continuum damage model. *International Journal of Pavement Engineering*, 11(6):459–476.